Thermal annealing characteristics of Si and Mg-implanted GaN thin films

J. S. Chan[a] and N. W. Cheung
Department of Electrical Engineering and Computer Sciences, University of California, Berkeley, California 94720

L. Schloss, E. Jones, W. S. Wong, N. Newman, X. Liu, and E. R. Weber
Department of Material Science and Mineral Engineering, University of California, Berkeley, California 64720

A. Gassman and M. D. Rubin
Lawrence Berkeley Laboratory, 1 Cyclotron Road, University of California, Berkeley, California 64720

(Received 8 December 1995; accepted for publication 13 March 1996)

In this letter, we report the results of ion implantation of GaN using ^{28}Si and ^{24}Mg species. Structural and electrical characterizations of the GaN thin films after thermal annealing show that native defects in the GaN films dominate over implant doping effects. The formation energies of the annealing induced defects are estimated to range from 1.4 to 3.6 eV. A 40 keV 10^{14} cm^{-2} Mg implant results in the decrease of the free-carrier concentration by three orders of magnitude compared to unimplanted GaN up to an annealing temperature of 690 °C. Furthermore, we have observed the correlation between these annealing-induced defects to both improved optical and electrical properties. © 1996 *American Institute of Physics.*[S0003-6951(96)05219-9]

The wide band-gap nitrides have generated significant research interest within the last few years for both their blue light-emitting and high-temperature properties.' In particular. gallium nitride (GaN) has been most heavily investigated. Major progress has been made in the areas of film growth,' p- and n-type doping[2–4] as well as device fabrication.[5-7] In addition, there have been reports on selective isolation and doping of GaN via implantation using various ion species, such as H, He, and N for isolation,[8] and Mg:P and Si for doping[9] In this letter, we report the annealing characteristics of Si and Mg implanted molecular beam epitaxy (MBE) grown GaN.

GaN thin films grown on basal sapphire substrates (α-Al_2O_3) by an ion-assisted MBE system were used as starting material in this study. A GaN buffer layer ~100 A thick was grown at a substrate temperature of 500 °C. Epitaxial growth was subsequently performed between 675 and 750 °C. A Kaufmann ion source was used to supply activated nitrogen.[10] After growth. the GaN samples were implanted with a conventional ion implanter, using SiF_4 gas and 4N pure Mg as the sources for the ^{28}Si and ^{24}Mg species. respectively. Annealing was performed in a diffusion furnace between *600* and 1078 °C. Structural changes were monitored via x-ray diffraction using a four-circle Siemens D5000 diffractometer employing a Cu $K\alpha$ tube and four-bounce Ge monochromator. Carrier activation was characterized with hot point probe and variable temperature Hall effect (VTHE) measurements.

Two sets of GaN/Al_2O_3 starting material were employed. Sample A (designated as "resistive") consists of an n-type undoped film 0.5 μm thick, with a resistivity ρ of 2 $\times 10^5$ Ω cm (carrier concentration $n_s = 3 \times 10^{13}$ cm^{-2}, mobility $\mu_s < 1$ cm^2 V^{-1} s^{-1}). Sample B (designated as "conductive") also consists of an undoped film *0.5* μm thick, but with $\rho = 39$ Ω cm ($n_s = 2 \times 10^{17}$ cm^{-2}, $\mu_s < 1$ cm^2 V^{-1} s^{-1}). The difference between samples A and B was presumed to be due to the in-grown concentration of shallow autodoping donor centers and deep-level defects.[11] Each sample was divided into three specimens: Si implanted. Mg implanted- and a control. The energies and Auences used for the Si double implant were 200 keV and 70 keV, 2×10^{13} cm^{-2} and 5 $\times$ 10^{12} cm^{-2}, respectively. An energy of 40 keV and a Auence of 10^{14} cm^{-2} were used for the Mg implant.

After implantation. a silicon nitride (Si_3N_4) cap layer ~1000 Å thick was deposited over the GaN layers using a Technics PECVD reactor prior to the furnace annealing step. The purpose of the Si_3N_4 cap was to prevent decomposition of the GaN layer," which becomes thermodynamically unstable at -- 800 °C and 1 atm." Each isochronal anneal was performed at atmospheric pressure in nitrogen for 1 h.

No change in the full width half-maximum (~20 arc min) and peak intensity of the (0002) x-ray rocking curve was observed after implantation and subsequent annealing up to 1000 °C. The intensity of the x-ray diffraction peak dropped sharply after annealing at 1000 °C. The thin film transformed from transparent to whitish in color, and became semi-insulating with a sheet resistance $R_s > 10^8$ Ω.

After annealing. HF *(49%* conc.) was used to remove the Si_3N_4 cap. Lithographically patterned van der Pauw structures were fabricated using a Veeco Ar ion-beam etcher, and Al contacts were deposited by a Veeco thermal evaporator. The contacts were sintered in an AG Associates 210T rapid thermal annealing (RTA) at 450 °C for 15 s in a nitrogen atmosphere prior to electrical characterization. A new Si_3N_4 cap was deposited on the GaN overlayer after each set of x-ray diffraction and Hall effect measurements.

Resistivity and VTHE measurements were performed between 25-300 K on both as-grown and annealed control samples to assess GaN bulk effects. The resistivity data of the unimplanted samples A and B on an Arrhenius plot (not shown) yielded two activation regions, one in the high-temperature region (> 100 K) and the other in the low-

[a]Electronic mail: cjames@vivante.eecs.berkeley.edu

 0003-6951/96/68(19)/2702/3/$10.00

TABLE I. Variable temperature Hall effect data for unimplanted GaN sample A and B.[a]

Sample	n (No./cm^3) measured at 300 K	Mobility at 300 K (cm^2 V^{-1}s^{-1})	ΔE_a(meV) from high-temperature region
A (as-grown)	$3.2\times10^{13}\pm1.7\times10^{13}$	1 ± 0.5	51.2 ± 1.3
A (annealed a 850 °C)	$3.0\times10^{16}\pm2.4\times10^{16}$	1 ± 0.8	26.4 ± 2.7
B (as-grown)	$2.0\times10^{17}\pm1.7\times10^{17}$	1 ± 0.9	23.4 ± 1.7
B (annealed a 850 °C)	$2.3\times10^{18}\pm1.6\times10^{16}$	28 ± 0.6	- 0

[a]See Reference 16 for extensive characterization results.

temperature region (< 100 K). This effect may be due to a transition from band conduction via shallow centers to hopping conduction via deep level defects at low temperatures.[11] Extraction of the carrier concentration of the Hall data in the high-temperature region of as-grown sample B gives an activation energy ΔE_a of 23.4 meV, assuming compensation due to deep levels. The free-carrier concentration of the 850 °C annealed control sample B is found to be constant at 2×10^{18} cm^{-3} and does not freeze out (measured to 5 K), a phenomenon consistent with either impurity band formation[14] or defect states resonant with the conduction band.[15] For control sample B, the mobility increased from 1 to 28 after annealing at 850 °C, indicating the dominance of electron transport via band conduction. The VTHE results are summarized in Table I (see Ref. 16 for extensive electrical characterization results).

Cathodoluminescence (CL) measurements were also performed on control sample B. The CL spectra shown in Fig. 1 revealed a 7Ximprovement in the band edge (365 nm) luminescence intensity after annealing at 850 °C, which has been shown previously by Lin e *al.*[17] However, we have also observed the simultaneous improvement of electrical characteristics as described above. In addition to the broad yellow emission spectra, a deep level peak centered at 420 nm was also observed. Its intensity increase 8X dwith annealing. Doping due to diffusion of Si from the annealing cap is believed not to be important in this study because control sampl es A and B, which were both isochronally annealed,

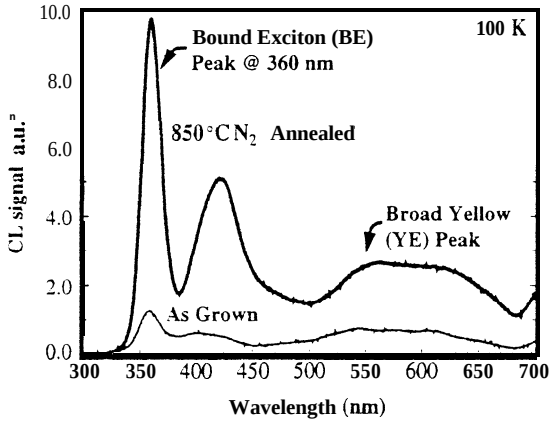

FIG. 1. The cathodoluminescence data measured at 100 K of the control GaN sample B ("conductive") as a function o f*annealing* temperature. The band edge (BE) luminescence peak improved 7X compared to th as-grown after a 850 °C anneal. and the electron carrier concentration an mobility increased from 2X 10^{17} to 2×10^{18} cm^{-3}, and 1 t o28 cm^2 V^{-1}s^{-1}, respectively.

have room-temperature carrier concentrations that are four orders of magnitude apart. Furthermore, Wilson et al. [18] reported Si diffusion in Si-implanted GaN to be negligible below 900 °C.

The implanted-layer resistivity was extracted using a two layer conductivity model," described by the following equations:

$$\sigma_{\text{tot}} = \frac{\sigma_s d_s + \sigma_b d_b}{d} = \frac{1}{Ptot}, \tag{1}$$

$$R_H = \frac{d(R_b\sigma_b^2 d_b + R_s\sigma_s^2 d_s)}{(\sigma_b d_b + \sigma_s d_s)^2}, \tag{2}$$

where ρ_{tot}, σ_{tot}, σ_b, σ_s, d, d_b, and d_s denote total resistivity measured, total conductivity, bulk (unimplanted) layer conductivity, implanted layer conductivity, total thickness, bulk thickness, and implanted laver thickness, respectively. R_H and R_b *are* the measured Hail coefficients for the combined two-layer structure and the bulk layer, whereas R_s is the extracted Hall coefficient for the implanted layer. The Hall carrier concentration and mobility of the implanted regions ca nbe extracted from R_s and σ_s ($n_s = -1/R_s$, $\mu_s = \sigma_s R_s$). *The* extraction process introduced. at most, a 10% error. The implantation thickness d_s, which is taken to be equal to the implant rang (*R,)* plus three times the longitudinal straggl e *(AR,),* was calculated to be -3600 Å for Si and 1000 Å for Mg based on TRIM simulations." Immediately after implantation with either Si or Mg, the carrier concentration dropped to below 10^{13} cm^{-3}, which is the lower detection limit for the Hall apparatus. Similar to the control samples. the carrier concentration of both the Si and Mg implanted samples increased with annealing temperature. In particular, for Mg-implanted sample B, a defect activation threshold occurred between 690 and 790 °C. Figure 2 shows a four orders of magnitude jump in electron carrier concentration from 10^{14} to 10^{18} cm^{-3} during this transition for the Mg-implanted sample. Likewise, the free-carrier concentration was suppressed by three orders of magnitude compared to the control sample prior to 690 "C. The Arrhenius plot of the electron concentration of control sample A versus annealing temperature yields a slope corresponding to a formation energy of 3.6 eV, while for sample B, the slope yields 1.4 eV.

The defect formation of the as-grown GaN films constituted a much stronger effect than the implantation itself. Because compensation resulted for both samples A and B immediately after implant, an implantation-induced deep level concentration of at leas 2X 10^{17} cm^{-3} (the background concentration of sample B) would be required in order to move

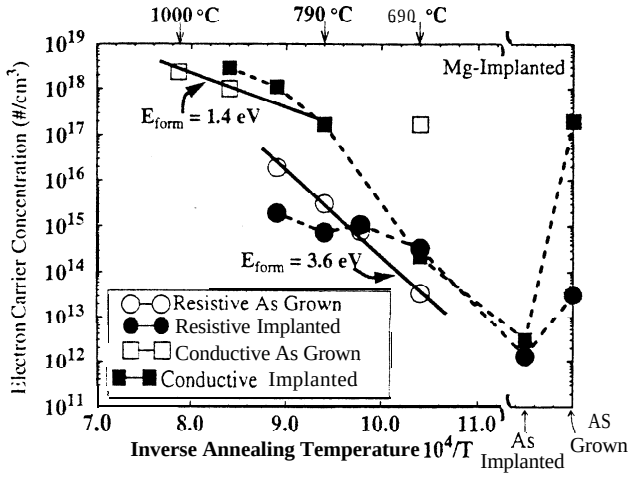

FIG. 2. Arrhenius plot of Hall electron carrier concentration measured at 300 K for the Mg-implanted samples in both sets A ("resistive") and B ("conductive";) as a function of inverse *annealing* temperarure (open symbols denote control samples; solid symbols denote implanted samples). E_{form} denotes formation energy of the shallow defects.

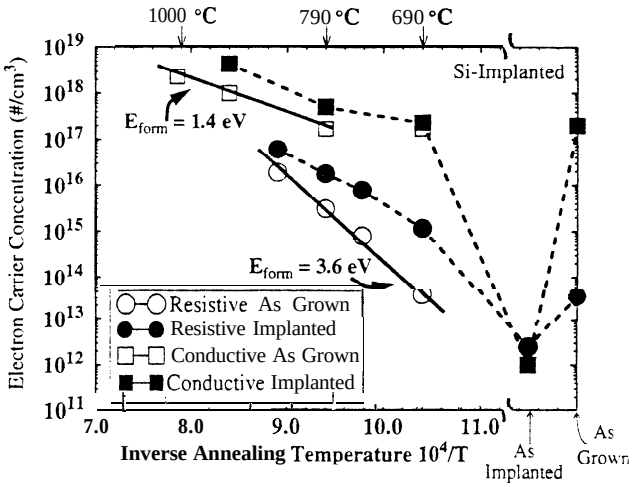

FIG. 3. Arrhenius plot of Hall electron carrier concentration measured at 300 K for the Si-implanted samples of both sets A ("resistive*') and B ("conductive") as a function of inverse *annealing* temperature (open symbols denote control samples; solid symbols denote implanted samples). E_{form} denotes formation energy of the shallow defects.

the Fermi level towards the midgap for both samples. In addition. a combination of vacancy generation. impurity depassivation and dopant activation with increasing annealing temperature could contribute to the electrical behavior of both the Mg and Si implanted samples. For example, the electron carrier concentration of both Si-implanted samples shown in Fig. 3 is at least 3X higher than the control after every annealing step above 690 "C. This result could be caused by electrical activation of Si dopant, which nonetheless is a secondary effect compared to the annealing-induced defects. Based on the CL results, the improved donor-bound excitonic peak (I_2) intensity could be linked to the increased shallow donor centers (possibly N vacancies) generated during the annealing process.

In summarv. our studv shows that the annealing-induced defect formation in as-grown GaN dominated over the dopine effect bv ion implantation. This defect is hypothesized to be-of a vacancy or a depassivated impurity nature. The formation energies for this defect are estimated to range from 1.4 to 3.6 eV. The physical origin of this defect is unknown. In the case of Mg-implanted GaN film. free-carrier concentration could be suppressed by three orders of magnitude with ion implantation up to 690 °C. The correlation between the annealing-induced defects and improved optical and electrical properties was observed, and will be further investigated.

We acknowledge Dr. E. E. Hailer of the LBL Material Science Division of LBL for access to the variable temperature Hall effect apparatus. This work benefited from the use of the UC-Berkeley Microfabrication Lab and the Integrated Materials Laboratory which is supported by the National Science Foundation. This research is supported in part by the Air Force Office of Scientific Research (AFOSR/JSEP) under Contract No. F49620-94-C-0038, and by the U.S. Department of Energy under Contract No. DE-AC03-76SF00098.

[1] H. Morkoç, S. Strite, G. B. Gao, and M. E. Lin, J. Appl. Phys. 76, 1363 (1994).
[2] S. Nakamura, T. Mukai. and M. Senoh, Jpn. J. Appl. Phys. 31. 2883 (1992).
[3] M. D. Rubin. N. Newman, J. S. Chan. T. C. Fu, and J. T. Ross. Appl. Phys. Lett. 64. 64 (1994).
[4] C. Wang and R. F. Davis. Appl. Phys. Lett. 63, 990 (1993).
[5] M. A. Khan. M. S. Shur. J. N. Kuznia. Q. Chen. J. Burm. and W. Schaff. Appl. Phys. Lett. 66. 1083 (1995).
[6] S. Nakamura. M. Senoh. and T. Mukai. Appl. Phys. Lett. 62. 2390 (1993).
[7] B. Goldenberg. J. D. Zook. and R. J. Ulmer, Appl. Phys. Lett. 62. 381 (1993).
[8] S. C. Binari. H. B. Dietrich, G. Kelner. and L. B. Rowland. J. Appl. Phys. 78, 3008 (1995).
[9] S. J. Pear-ton. C. B. Vartuli. J. C. Zolper, C. Yuan. and R. A. Stall. Appl. Phys. Lett. 67. 1435 (1995).
[10] N. Newman. T. C. Fu, X. Liu. Z. Liliental-Weber. M. D. Rubin. J. S. Chan. E. Jones. J. T. Ross. I. Tidswell, K. M. Yu. N. W. Cheung. and E. R. Weber. Mater. Res. Soc. Symp. Proc. 339. 383 (1994).
[11] R. J. Molnar. T. Lei. and T. D. Moustakas, Appl. Phys. Lett. 62. 72 (1993).
[12] C. Stolte. in *Semiconductors and Semimetals* (Academic. Orlando. FL. 1984). Vol. 20.
[13] N. Newman. J. T. Ross. and M. D. Rubin. Appl. Phys. Lett. 62, 1242 (1993).
[14] A. G. Milnes. *Deep Impurities in Semiconductors* (Wiley. New York. 1973).
[15] W. M. Chen. P. Dreszer. A. Prasad. and A. Karpieski, J. Appl. Phys. 76. 600 (1994).
[16] J. S. Chan. Ph.D. thesis, College of Engineering, UC-Berkeley, 1995.
[17] M. E. Lin, B. N. Sverdlov, and H. Morkoç, Appl. Phys. Lett. 63. 3625 (1993).
[18] R. G. Wilson, S. J. Pearton, and C. R. Abernathy, Appl. Phys. Lett. 66. 2238 (1995).
[19] D. C. Look, *Electrical Characterization of GaAs Materials and Devices* (Wiley, New York, 3989).
[20] J. F. Ziegler and J. P. Biersack, TRIM-W (Pergamon, New York, 1990).